# NUMERICAL STUDY AND ANALYSIS OF COMPOSITE STRUCTURES WITH GRADED FOAM

**Andrejs Kovalovs[1], Pavel Akishin[1], Vanesa Dhalivala[2], Ugis Cabulis[2]**
[1]Riga Technical University, Latvia; [2]Latvian State Institute of Wood Chemistry, Latvia
andrejs.kovalovs@rtu.lv, pavels.akisins@rtu.lv, vanesa.dhalivala@kki.lv, ugis.cabulis@kki.lv

**Abstract.** The aim of this study is to analyse the behaviour of a composite structure with an internal core made of graded polymer foam. Functionally graded foam is an innovative class of materials mechanical properties or chemical composition of which change in a prescribed direction of the material. The object of the study is a simplified model of a full-size helicopter blade in a composite box plate configuration. The graded properties of the core vary across the structure's width. It is assumed that the use of graded foam can influence the blade stiffness, including both bending and torsional stiffnesses. In addition, the centres of mass and torsion of the structure are studied. The influence of the distribution law of functionally graded foam on the stiffness characteristics of composite structures was calculated using ANSYS software. Two types of rigid foams are used in these analyses: rigid polyurethane (RPU) foam and closed-cell rigid foam based on polymethacrylimide (Rohacell). The polyurethane foam was produced from renewable resources, as well as environmentally friendly catalysts and foaming agents with different densities. To model the graded foam as the rotor blade core, the foam density and mechanical properties of RPU foam were tested. The mechanical properties of Rohacell foam with different densities were taken from the manufacturer's data sheet. It was established that graded polyurethane foam has lower mechanical properties than Rohacell foam. Consequently, the influence of graded polymer foam on the stiffness characteristics of composite structures is negligible. In contrast, the use of Rohacell foam has a significant effect on stiffness.

**Keywords:** functionally graded foam, static, analysis, ANSYS.

## Introduction

The high vibration levels during a helicopter flight negatively affect structural integrity and passenger comfort. Introduction of active control systems into the helicopter rotor blade reduces vibrations during flight [1]. The development of piezoelectric macrofibre composite actuators (MFCs) has enabled the study of new approaches to blade control, improved aerodynamic performance, and reduced vibrations. One such approach is active twist control, which regulates blade twist using piezoelectric actuators embedded in the blade skin. The piezoelectric fibres in the actuator on the upper and lower blade surfaces are oriented at ± 45°, producing dynamic blade twisting when the actuators are activated, thereby improving aerodynamic performance [2; 3].

At the same time, advances in mechanical and aerospace engineering continue to drive demand for new materials with unique properties. In recent years, a new class of composite materials known as functionally graded materials (FGMs) has emerged. FGMs are characterised by continuous variation in structure, mechanical properties, or chemical composition along a prescribed direction. This gradual variation in material properties enables the development of components with performance capabilities surpassing those of conventional composites, thereby broadening their applicability in advanced engineering systems. At present, FGMs have been developed with gradients in chemical, mechanical, magnetic, thermal, electrical, and other properties. Depending on the smoothness of the property variation, these materials are classified as either discrete or continuous gradient materials [4]. Gradient systems are complex objects, making their structure and properties difficult to study, which explains the limited number of works in this area.

One of the least-studied types of graded materials is polymer foam [5]. Due to their combination of mechanical and thermal properties, low weight, and cost, polymer foams are widely used in engineering applications. The concept of graded foam has become particularly prominent in problems related to energy absorption [6]. Polymer foams with a density gradient along a prescribed direction can enhance the impact resistance of foam structures [7].

The development and application of functionally graded foams as filler inside the rotor blades opens up the possibility of changing their stiffness characteristics, as well as changing the position of the elastic axis and the centre of gravity of the blade. This, in turn, contributes to the more efficient control of the rotor blades during flight, requiring less electrical energy to implement active twist. The objective of this study is to analyse the behaviour of a simplified model of a full-size helicopter blade with an internal core made of graded polymer foam. This study serves as a preliminary investigation to understand the

DOI: 10.22616/ERDev.2026.25.TF147

behaviour of a simplified finite element model before analysing a realistic rotor blade containing functionally graded polymer foam. It is assumed that incorporating functionally graded foam can influence the blade stiffness, including both bending and torsional stiffnesses. The primary aim of this research is to examine how different distributions of graded foam within the composite structure affect the stiffness characteristics and the locations of the centre of gravity and the elastic axis. In addition, understanding the influence of graded foam on the investigated parameters is essential when addressing the blade optimal design problem, where these parameters are considered as design constraints. Finally, the application of piezoelectric MFC actuators and a composite structure with graded foam within is considered.

## Materials and methods

Two foam materials are considered in the present research for use in aviation constructions: rigid polyurethane foam and closed-cell rigid foam based on polymethacrylimide (PMI) chemistry, ROHACELL WF. RPU foam was developed from renewable bio-based components and recyclable components. Specimens of RPU foam were manufactured with nominal densities 30, 40, 50, 60, and 70 kg·m$^{-3}$ and experimentally investigated under tension. For the tensile tests, the specimens were prepared according to ISO 1926 by using an Instron testing machine. At least six dog-bone-shaped specimens were fabricated and tested for each density. The experimental tests were performed at room temperature using a cross-head displacement rate of 1 mm·m$^{-1}$in. Fig. 1a presents the average Young's modulus of elasticity for RPU foam manufactured at different densities.

The mechanical properties of Rohacell foam with different densities were taken from the manufacturer's data sheet of EVONIK Company, which produces a ROHACELL WF foam core especially for the aerospace industry [8]. Based on the website data, the foam density ranges from 52 to 300 kg·m$^{-3}$, while the Young's modulus ranges from 75 to 580 MPa. Fig. 1 illustrates the correlation between density and elastic modulus. It is observed that the dependence of the elastic modulus on density is linear.

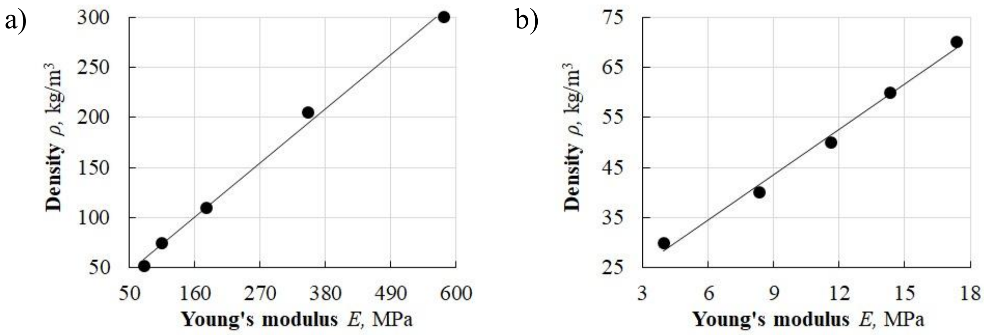


Fig. 1. **Correlation between density and elastic modulus:** a – RPU foam; b – Rohacell WF foam

Thus, two graded foam material models with low and high Young's modulus and density are chosen for the parametric study of the composite structure. In the RPU foam, Young's modulus can vary from 3.9 to 17.4 MPa, and the density varies from 30 to 70 kg·m$^{-3}$. In the Rohacell WF foam, Young's modulus can vary from 75 to 580 MPa, and the density varies from 52 to 300 kg·m$^{-3}$. Note that Poisson's ratio remains constant for each type of foam material specified by the manufacturer. Therefore, following this study and the approaches used in [9], Poisson's ratio is assumed to be 0.3 and is not varied according to the power law.

Across the width of the structure, the polymer foam Young's modulus and density vary according to a power-law function [7]:

$$E(x) = \left(E_R - E_L\right)\cdot\left(1 - \frac{x}{W}\right)^p + E_L, \quad (1)$$

$$\rho(x) = \left(\rho_R - \rho_L\right)\cdot\left(1 - \frac{x}{W}\right)^p + \rho_L, \quad (2)$$

where $L$, $R$ – subscripts denoting the polymer foam properties on the left and right sides, respectively;
$E$, $\rho$ – correspond to the Young's modulus and density of the foam;
$p$ – represents power-law index.

The highest numerical values of the investigated material properties correspond to the Young's modulus $E_R$ and density $\rho_R$. The lowest numerical values of the investigated material properties correspond to the Young's modulus $E_L$ and density $\rho_L$.

The Shear modulus $G$ of the polymer foam is defined as:

$$G(x) = \frac{E(x)}{2 \cdot (1+\nu)}, \tag{3}$$

where $\nu$ – denotes the Poisson's ratio, which is constant.

Fig. 2 depicts an example of Model 2, showing how Young's modulus and density change as a function of the power-law index $p$. It is seen that the left side corresponds to the maximal value of the Young's modulus and density.

The cross-section of the composite structure examined in this study is presented in Fig. 3. Fig. 3 illustrates the cross-sectional dimensions selected for the full-scale rotor blade BO105. The composite box-plate has a width $W$ = 0.3 m, a thickness $H$ = 0.03 m, and a length $B$ = 3.75 m. The internal core is modelled as a graded polymer foam which properties vary smoothly across the structure's width. Unidirectional (UD) glass fiber-reinforced plastic (GFRP) is used as the skin material. The skin consists of four glass fiber layers arranged in a [+45/-45] reinforcement scheme, with a total thickness of 0.5 mm [10].

The material properties of the UD GFRP material are as follows: Young's moduli $E_x$ = 45.166 GPa, $E_y$ = $E_z$ = 11.981 GPa, Poisson's ratios $\nu_{xy}$ = $\nu_{xz}$ = 0.238, $\nu_{yz}$ = 0.325, shear moduli $G_{xy}$ = $G_{xz}$ = 4.583 GPa, $G_{yz}$ = 1.289 GPa, and density $\rho$ = 2008 kg·m$^{-3}$ [10].

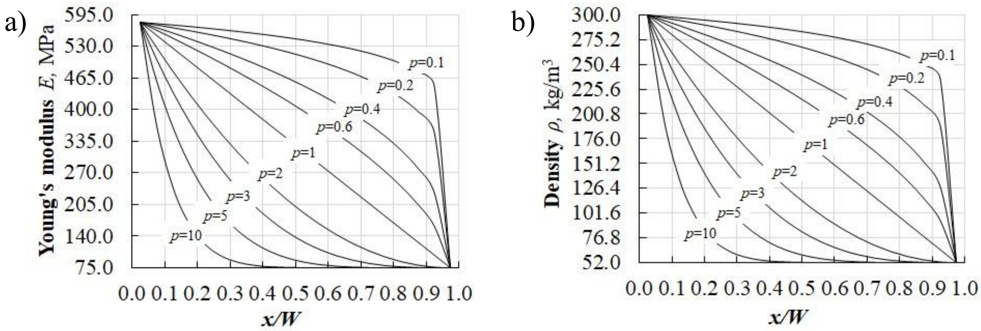


Fig. 2. **Variations for different values of the power-law index *p*:**
a – Young's modulus; b – density

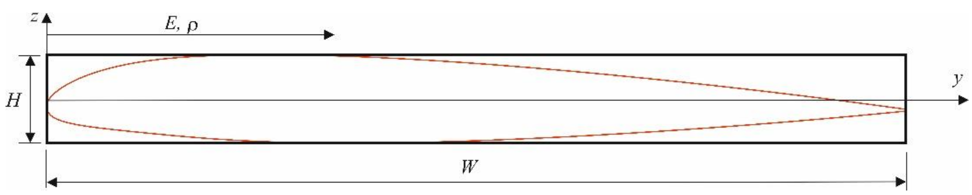


Fig. 3. **Cross-section of full-size rotor blade airfoil inside of composite box plate**

A three-dimensional finite element (FE) model of the composite box-plate was developed using ANSYS 16.0 software. Linear 4-node SHELL181 elements were employed to model the multilayered composite skin, while linear 8-node SOLID185 elements were used for the graded foam core. Prior to the numerical analysis, a mesh-convergence study was performed to ensure acceptable solution accuracy. Finally, 60 layers were used to model the graded foam in the finite element model (Fig. 4). Each colour in the FE model corresponds to a set of material properties in the beam cross-section, varying with the power–law index $p$ along the width. The final FE model consisted of approximately 270,000 elements. The structure was constrained using a clamped boundary condition.

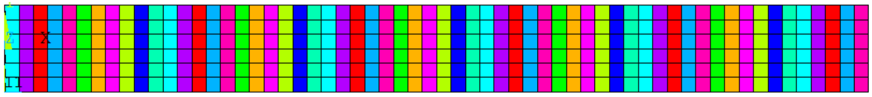

Fig. 4. **Cross-section of the finite element model, illustrating the graded polymer-foam core**

The main cross-sectional parameters of a helicopter blade used in dynamic and flutter analyses are lag-bending stiffness, flap-bending stiffness, and torsional stiffness. In addition, the mass of the structure $m$, the location of the centre of gravity $y_{cg}$, and the location of the elastic axis $y_{ea}$ are studied. The structural parameters, including the composite structure mass $m$ and the centre of gravity $y_{cg}$, can be obtained from ANSYS calculations. Determining the elastic axis location $y_{ea}$ requires several static analyses in which two independent forces are applied to opposite sides of the cross-section. Using the resulting displacements from each load case, the location of the elastic axis $y_{ea}$ can be identified. The procedure for determining the location of the elastic axis $y_{ea}$ is presented in [11].

The lag and flap bending stiffnesses were obtained from the following equation [12]:

$$EI = \frac{PL^3}{3\Delta}, \tag{4}$$

where $P$ – applied force;
$L$ – length of the structure;
$\Delta$ – maximum displacement of the composite box-plate (Fig. 5).

Torsional stiffness was calculated by means of the following equation [12]:

$$GJ = \frac{2PlL}{\alpha}, \tag{5}$$

where $P$ – applied force;
$L$ – length of the structure;
$l$ – distance between the point of force application and the elastic axis;
$\alpha$ – angle of twist (Fig. 5).

In the finite element model, the piezoelectric effect was modelled using the thermal analogy. It is assumed that temperature strains and piezoelectric strains are equal, and the electric field is replaced by an equivalent temperature field. The piezoelectric coefficients are replaced by thermal expansion coefficients. Using temperature instead of voltage allows the piezoelectric effect to be modelled using shell elements that describe the piezoelectric actuators [13].

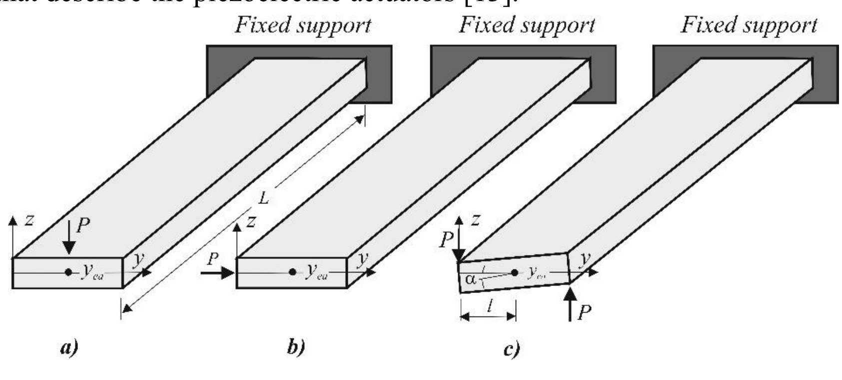


Fig. 5. **Scheme for determining:** a – flap bending; b – lag bending; c – torsional stiffnesses

## Validation study

To verify the accuracy of modelling a functionally graded material in ANSYS, the static bending displacement of a graded beam with a distributed load $q$ is analysed. The material's graded properties are assumed to vary continuously through the beam thickness. The bottom surface of the beam is composed of aluminium, with an elastic modulus $E_m$ = 70 GPa and Poisson's ratio $v_m$ = 0.3. The top surface is made of alumina ($Al_2O_3$), characterised by an elastic modulus $E_c$ = 380 GPa and Poisson's ratio $v_c$ = 0.3. The material properties are graded continuously through the beam thickness. The total beam thickness is $h = 0.1$ m. Two geometric configurations are considered, corresponding to length-to-height ratios $L/h = 5$ and 20. The graded beam was constrained using a clamped boundary condition.

The maximum dimensionless vertical displacement is calculated as:

$$w^* = \frac{100h^3 E_m}{qL^4} w, \tag{6}$$

where $w^*$ denotes the maximal vertical displacement of the graded beam and $q$ is the uniformly distributed load of 100 N·m$^{-12}$. Linear 8-node SOLID185 elements were used to model the graded beam. The beam thickness was discretized into 20 layers to represent the continuous variation of the graded material properties. Numerical results obtained in ANSYS are compared with the results reported by Nguyen et al. [14]. Table 1 presents the results, which show good agreement with the analytical solution.

Table 1

**Maximum dimensionless displacements**

| ***L/h*** | **Source** | **Power law index** | | | | |
|---|---|---|---|---|---|---|
| | | $p = 0$ | $p = 1$ | $p = 2$ | $p = 5$ | $p = 10$ |
| 5 | Nguyen et.al [14] | 28.5743 | 56.2359 | 71.7607 | 86.1492 | 95.7903 |
| | Present (ANSYS) | 28.3710 | 56.3628 | 72.5200 | 87.1037 | 96.6060 |
| 20 | Nguyen et.al [14] | 27.6087 | 54.6051 | 69.4911 | 82.4327 | 91.1965 |
| | Present (ANSYS) | 27.5743 | 55.2257 | 70.9010 | 84.1201 | 92.7632 |

**Results and discussion**

Fig. 6 shows the dependence of the investigated parameters on the power-law index $p$. Model 1 means the composite box plate is used with the graded RPU foam. Model 2 means that the composite box plate is used with the graded Rohacell WF foam. The percentage change between the minimal and maximal values of the parameters obtained is presented in Table 2.

When $p = 0$, the foam in the composite box plate is equal to the maximal value of the Young's modulus and density. According to the material-distribution law, the mass of the composite structure decreases as the power-law index $p$ increases. The reduction in mass exceeds 23.2% for Model 1 and 55.3% for Model 2, respectively (Fig. 6a). The change in the structural mass influences the location of the centre of gravity $y_{cg}$; as a result, $y_{cg}$ shifts to the left (Fig. 6b). The largest variation of the location is observed at $p = 2$. However, the percentage change in the centre of gravity location for Model 1 is only 5.7%, whereas in Model 2 it is 19.8%. A similar trend is observed for the location of the elastic axis $y_{ea}$, which shifts to the left (Fig. 6c). For Model 1, the percentage difference between the maximum and minimum locations is only 0.7%. Model 2 shows a similarly small variation of 6.4%. It should be noted that at $p = 0$, the foam exhibits isotropic properties, and in this case, the locations of the centre of gravity $y_{cg}$ and the elastic axis $y_{ea}$ coincide with the geometric centre of the structure, as shown in Fig. 6b and Fig. 6c, respectively. The decrease of the elastic modulus along the width of the structure $W$ with increasing $p$ leads to a reduction in the lag bending, flap bending, and torsional stiffnesses (Figs. 6d, 6e, and 6f, respectively). The percentage change in lag and bending stiffnesses in Model 1 does not exceed 2%, but the torsional stiffness changes by 7.6%. Compared with Model 1, Model 2 exhibits substantially larger percentage changes in stiffness characteristics as the power–law index $p$ increases. The lag–bending stiffness decreases by 31.9%, the flap–bending stiffness decreases by 21.7%, and the torsional stiffness decreases by 13.2% with increasing $p$.

Compared with Models 1 and 2, the graded foam from RPU has the least influence on the investigated parameters of the composite box plate. The results of the study are presented in Fig. 6. The additional mass of the piezoelectric actuators increased the composite structure's mass to 3.2 kg (Fig. 6a). The increased mass of the composite structure reduced the shifts of the centre of gravity $y_{cg}$ and the elastic axis $y_{ea}$, depending on the power–law index $p$, achieving 13.7 and 5.3%, respectively (Fig. 6b and Fig. 6c). The use of piezoelectric actuators in Model 2 leads to an increase in its stiffness characteristics. The average lag-bending stiffness increases by 1.9 times, the average flap-bending stiffness increases by 1.6 times, and the average torsional stiffness increases by 1.3 times. At the same time, the high percentage change in the structure stiffness characteristics with respect to power–law index $p$ is preserved, as in Model 1 without piezoelectric actuators. The lag–bending, flap–bending, and torsional stiffnesses decrease by 20.8, 11.9, and 17.0%, respectively, with increasing $p$. The greatest effect on these parameters is observed in Model 2, which incorporates Rohacell WF foam properties. Thus, Model 2 was chosen for further research and analysis of the composite structure with piezoelectric actuators.

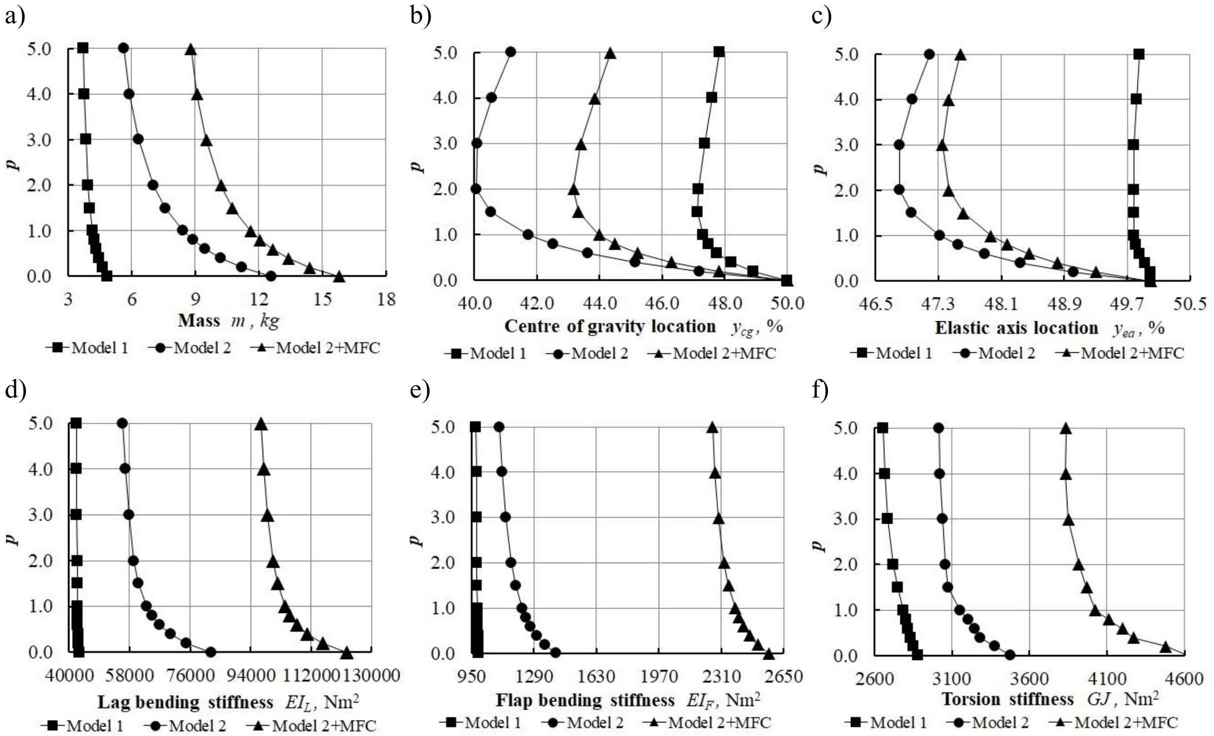


Fig. 6. **Parametric study of composite box plate**

Table 2

**Percentage change between the maximal and minimal values of the investigated parameters**

| Type of model | $m$, kg·m$^{-1}$ | $y_{cg}$, %c | $y_{ea}$, %c | $EI_{Lag}$, Nm$^2$ | $EI_{Flap}$, Nm$^2$ | $GJ$, Nm$^2$ |
|---|---|---|---|---|---|---|
| Model 1 | 23.2% | 5.7% | 0.7% | 1.6% | 1.5% | 7.6% |
| Model 2 | 55.3% | 19.8% | 6.4% | 31.9% | 21.7% | 13.2% |
| Model 2 + MFC | 44.2% | 13.7% | 5.3% | 20.8% | 11.9% | 17.0% |

An additional study was conducted to investigate the influence of the twist angle of the composite structure as a function of the power-law index $p$, using Model 2 with MFC actuators (Fig. 7). At the minimum value $p = 0$, the twist angle $\alpha$ of the Model 2 produced by the activated MFC actuators is 2.64°. At the maximum value $p = 5$, the twist angle reaches only 2.83°, which corresponds to an increase of just 6.5%.

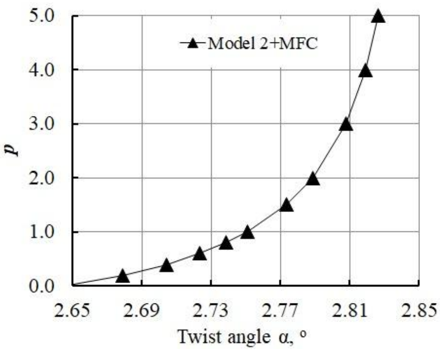


Fig. 7. **Influence of the power–law index $p$ on the twist angle**

## Conclusions

1. The use of graded foam in Model 2, based on Rohacell WF foam properties, has the greatest influence on the stiffness parameters of the lightweight composite structure, compared with Model 1, which uses RPU foam. In Model 2, the application of graded foam changes the flap-bending, lag-bending, and torsional stiffnesses by approximately 13-32% as the power-law index $p$ increases. Piezoelectric actuators added to Model 2 increase the construction's stiffness and reduce shifts in the centre of gravity and the elastic axis locations. Behaviour or investigated parameters: Model 2 with MFC actuators shows a similar trend to Model 1.
2. The addition of piezoelectric actuators to Model 2 increases the stiffness of the structure and reduces the shift of the centre of gravity and the location of the elastic axis. The behaviour of the investigated parameters in Model 2 with MFC actuators follows a trend similar to that observed in Model 1.
3. The percentage change in twist angles for composite structures with graded foam and MFC actuators between the minimum and maximum values of $p$ is 6.5%. A graphical representation of the influence of the power-law index $p$ on the twist angle shows that an increase in the power-law index $p$may lead to a larger twist angle.

## Acknowledgements

This research was funded by the Latvian Council of Science, project "Smart twisting active rotor blades with a functionally graded foam core (SmarTARB)" No. lzp-2023/1-0587.

## Author contributions

Conceptualization, A.K., and U.C.; methodology, A.K.; validation A.K.; formal analysis, A.K. and U.C.; finite element investigation, P.A.; experiment, V.D.; data curation, writing – original draft preparation, A.K.; writing – review and editing, A.K. and U.C.; visualization, A.K. and U.C.; project administration, A.K.; funding acquisition, A.K. All authors have read and agreed to the published version of the manuscript.

## References

[1] Friedmann P.P., Millott T.A. Vibration Reduction in Rotorcraft Using Active Control: A Comparison of Various Approaches. Journal of Guidance, Control, and Dynamics, Vol.18, 1995, pp. 664-673.
[2] Van der Wall B.G., Lim J.W., Riemenschneider J., Kalow S., et al. New smart twisting active rotor (STAR): Pretest predictions. CEAS Aeronautical Journal, Vol. 15, 2024, pp. 721-750.
[3] Han D., Zhang Y. Research progress in active twist rotor. Acta Aerodynamica Sinica, Vol.43, 2025, pp. 52-66.
[4] Saleh B., Jiang J., Fathi R., et al. 30 years of functionally graded materials: an overview of manufacturing methods, applications and future challenges. Composites Part B: Engineering, Vol. 201, 2020, 108376.
[5] Suethao S., Shah D. U., Smitthipong, W. Recent Progress in Processing Functionally Graded Polymer Foams. Materials, Vol. 13(18), 2020, 4060.
[6] Xu F., Zhang X., Zhang H. A review on functionally graded structures and materials for energy absorption. Engineering Structures, Vol. 171, 2018, pp. 309-325.
[7] Li S., Li Q.M., Tse K.M., Pang, T. Functionally graded foam materials for head impact protection. Thin-Walled Structure, Vol. 203, 2024, 112193.
[8] EVONIK Homepage. [online] [31.05.2025] Available at: https://performance-foams.evonik.com/en/downloads/product-information
[9] Ruan M., Wang Z.M. Transverse vibrations of moving skew plates made of functionally graded material. Journal of Vibration and Control. 2016, 22(6), pp. 3504-3517.
[10] Kovalovs A., Barkanov E., Ruchevskis S., Wesolowski M. Modeling and Design of a Full-Scale Rotor Blade with Embedded Piezocomposite Actuators. Mechanics of Composite Materials, Vol. 53, 2017, pp. 179-192.
[11] Kovalovs A. Modelling, Parametric Study, and Optimisation of 3D Model-Scale Helicopter's Rotor Blade with Piezoelectric Actuators. Applied Sciences, Vol.16, 2026, 1319.

[12] Riemenschneider J., Keye S., Wierach P., and Mercier Des Rochettes, H. Overview of the common DLR/ONERA project active twist blade (ATB). In: Proceedings of the 30th European rotorcraft forum, Marseille, France (2005), pp. 273-281.
[13] Barkanov E., Kovalovs A., Anoshkin A., Pisarev P. An Application of Thermal Analogy in Active Control Problems. In Advanced Materials Modelling for Mechanical, Medical and Biological Applications; Altenbach, H., Eremeyev, V.A., Galybin, A., Vasiliev, A., Eds., Advanced Structured Materials; Springer: Berlin/Heidelberg, Germany, 2022; Volume 155, pp. 51-62.
[14] Nguyen H.N. Hong T.T., Vinh P.V., Thom D.V. An Efficient Beam Element Based on Quasi-3D Theory for Static Bending Analysis of Functionally Graded Beams. Materials, Vol. 12(13), 2019, 2198.